

Magic Gems: A Polyhedral Framework for Magic Squares

Connecting Combinatorics, Geometry, and Linear Algebra

Kyle Elliott Mathewson
Faculty of Science, University of Alberta
 kyle.mathewson@ualberta.ca

December 11, 2025

Abstract

We introduce *Magic Gems*, a geometric representation of magic squares as three-dimensional polyhedra. By mapping an $n \times n$ magic square onto a centered coordinate grid with cell values as vertical displacements, we construct a point cloud whose convex hull defines the Magic Gem. Building on prior work connecting magic squares to physical properties such as moment of inertia, this construction reveals an explicit statistical structure: we show that magic squares have vanishing covariances between position and value. We develop a covariance energy functional—the sum of squared covariances with row, column, and diagonal indicator variables—and establish rigorously for $n = 3$ (via exhaustive enumeration) that its zeros correspond precisely to magic squares. Large-scale sampling for $n = 4, 5$ (460+ million arrangements) provides strong numerical evidence that this characterization extends to larger orders. Perturbation analysis demonstrates that magic squares are isolated local minima. The representation is invariant under dihedral symmetry D_4 , yielding canonical geometric objects for equivalence classes.

Keywords: Magic squares, convex polyhedra, covariance, energy landscape, combinatorial geometry

1 Introduction

Magic squares have fascinated mathematicians, artists, and mystics for millennia [11]. The oldest known example, the *Lo Shu* square, appears in Chinese legend dating back to 2800 BCE and remains the unique (up to symmetry) 3×3 magic square using the integers 1 through 9. Despite this ancient pedigree and centuries of intensive study [2], magic squares continue to yield new mathematical insights, with recent work connecting them to algebraic structures, eigenvalue problems, and statistical mechanics.

Definition 1.1 (Magic Square). An $n \times n$ *magic square* is an arrangement of the integers $1, 2, \dots, n^2$ in a square grid such that the sum of each row, each column, and both main diagonals equals the *magic constant*

$$M(n) = \frac{n(n^2 + 1)}{2}. \quad (1)$$

In this paper, we develop a geometric perspective on magic squares by representing them as three-dimensional polyhedra, which we call *Magic Gems*. The construction arises from a natural physical analogy: imagine placing checkers on an $n \times n$ board, where the height of each stack corresponds to the number occupying that cell. This creates a “topography” over the grid, and centering this configuration in three-dimensional space yields a point cloud whose convex hull defines the Magic Gem. This geometric approach complements prior work by Loly and collaborators on the physical properties of magic squares [6, 7, 9].

The central insight of this work is that the defining algebraic property of magic squares—equal row, column, and diagonal sums—manifests geometrically as a precise statistical condition. Specifically, we show that magic squares are characterized by the vanishing of a covariance energy functional that measures correlations between spatial position and assigned value across all four structural directions (rows, columns, and both diagonals). This energy characterization builds on earlier work connecting magic squares to physical properties such as moment of inertia [7], providing an explicit statistical framework that bridges classical combinatorics and multivariate analysis.

1.1 Main Contributions

This paper develops the Magic Gem framework through several interconnected results. We begin by formalizing the construction of Magic Gems from magic squares and establishing that symmetry-equivalent squares yield geometrically identical polyhedra, thus providing a canonical geometric representative for each equivalence class under the dihedral group D_4 .

Our main theoretical contribution is the Energy Characterization Theorem (Section 3.13), which establishes that magic squares correspond to zeros of a covariance energy functional. We prove this result rigorously for $n = 3$ via exhaustive enumeration, and provide strong computational evidence for larger orders. This result extends the physical interpretation of magic squares initiated by Loly [7], who showed that the moment of inertia tensor of a magic square (treating entries as masses) exhibits special invariance properties. Our covariance formulation makes this connection explicit and enables systematic perturbation analysis, confirming that magic squares are isolated points in the arrangement space.

We complement these theoretical results with extensive computational experiments on magic squares of orders three, four, and five. These experiments validate our theoretical predictions and reveal the geometric structure of both the Magic Gems themselves and the broader space of arrangements in which they reside. The rarity of magic squares—approximately one in 45,000 random 3×3 arrangements—corresponds to their isolation as zero-covariance configurations in a landscape where generic arrangements exhibit substantial covariance. An interactive web application for exploring Magic Gems is available at <https://kylemath.github.io/MagicGemWebpage/>.

1.2 Paper Organization

The remainder of this paper proceeds as follows. Section 2 reviews classical results on magic squares and establishes notation for the geometric and statistical concepts we employ. Section 3 presents the Magic Gem construction, proves the Energy Characterization Theorem, and develops the perturbation analysis framework. Section 4 describes our computational experiments, validating theoretical predictions and exploring the structure of the arrangement space for $n = 3$, 4, and 5. Section 5 interprets our findings and discusses connections to related areas. Finally, Section 6 summarizes our contributions and outlines directions for future research.

2 Background

This section establishes the mathematical foundations for our work, reviewing classical results on magic squares and introducing the geometric and statistical concepts that underpin the Magic Gem framework.

2.1 Magic Squares: Classical Results

The enumeration of magic squares reveals a rapid growth in complexity with the order n [12]. For $n = 3$, there exist exactly eight magic squares, all related by rotations and reflections, yielding a single essentially different magic square—the Lo Shu. The situation changes dramatically

for larger orders: $n = 4$ admits 7,040 magic squares forming 880 equivalence classes under the dihedral group, while $n = 5$ yields approximately 275 million magic squares comprising roughly 34 million equivalence classes. This explosive growth poses significant challenges for enumeration and classification, motivating the search for structural insights that transcend explicit construction.

The magic constant $M(n) = n(n^2 + 1)/2$ admits a simple derivation from first principles. The sum of all entries equals $\sum_{k=1}^{n^2} k = n^2(n^2 + 1)/2$, which must be distributed equally among the n rows, yielding $M(n)$ per row. The same argument applies to columns, and the diagonal constraints provide additional structure that severely restricts the space of valid configurations.

Classical construction methods provide algorithmic approaches to generating magic squares of various orders [2]. The Siamese method, attributed to de la Loubère, constructs magic squares for odd n by starting in the middle of the top row and moving diagonally up-right, wrapping around edges and moving down when blocked. For doubly-even orders (n divisible by 4), one fills the grid sequentially and then swaps diagonal elements with their complements. Singly-even orders ($n = 4k + 2$) require more sophisticated techniques combining quadrant-based construction with targeted transpositions. These methods demonstrate that magic squares exist for all $n \geq 3$, though they produce only a tiny fraction of all possible magic squares for larger orders.

2.2 Symmetry and the Dihedral Group

The dihedral group D_4 acts naturally on $n \times n$ grids through rotations and reflections [1]. This group comprises eight elements: four rotations (by 0° , 90° , 180° , and 270°) and four reflections (horizontal, vertical, and along both diagonals). Since the magic square conditions treat rows, columns, and diagonals symmetrically under these operations, D_4 permutes magic squares among themselves.

Proposition 2.1. *If S is a magic square, then $g \cdot S$ is also a magic square for any $g \in D_4$.*

Proof. The D_4 action preserves the set of row sums, column sums, and diagonal sums, merely permuting which lines play which roles. Since the action also preserves the set of entries $\{1, \dots, n^2\}$, it maps magic squares to magic squares. \square

This symmetry motivates the notion of *essentially different* magic squares: two squares are essentially the same if one can be obtained from the other by a D_4 transformation. For $n = 3$, all eight magic squares form a single equivalence class, while larger orders admit multiple classes with distinct structural properties.

2.3 Convex Hulls and Polyhedra

The convex hull of a finite point set $P \subset \mathbb{R}^d$ is the smallest convex set containing P , equivalently characterized as the set of all convex combinations of points in P :

$$\text{conv}(P) = \left\{ \sum_{i=1}^k \lambda_i p_i : p_i \in P, \lambda_i \geq 0, \sum_i \lambda_i = 1 \right\}.$$

For finite point sets in \mathbb{R}^3 , the convex hull is a convex polyhedron whose vertices form a subset of the original points. The remaining points lie in the interior or on faces of the polyhedron.

Key geometric quantities associated with a convex polyhedron include its volume, surface area, and the number of vertices, edges, and faces. These invariants provide a coarse characterization of the polyhedron's shape and will serve as descriptors for comparing Magic Gems across different arrangements.

2.4 Covariance and the Moment of Inertia

For a discrete collection of points $\{(\mathbf{x}_i)\}_{i=1}^N$ with positions $\mathbf{x}_i \in \mathbb{R}^d$, the covariance matrix captures the second-order statistical structure:

$$\Sigma_{jk} = \frac{1}{N} \sum_{i=1}^N (x_{i,j} - \bar{x}_j)(x_{i,k} - \bar{x}_k), \quad (2)$$

where $\bar{x}_j = \frac{1}{N} \sum_i x_{i,j}$ denotes the mean of the j -th coordinate. When the point cloud is centered so that $\bar{\mathbf{x}} = \mathbf{0}$, this simplifies to $\Sigma_{jk} = \frac{1}{N} \sum_i x_{i,j} x_{i,k}$.

The diagonal entries Σ_{jj} measure the variance along each coordinate axis, while the off-diagonal entries Σ_{jk} ($j \neq k$) measure the covariance between coordinates. A zero off-diagonal entry indicates that the corresponding coordinates are uncorrelated: knowing one provides no linear information about the other.

Closely related is the moment of inertia tensor from classical mechanics. For point masses $\{(m_i, \mathbf{x}_i)\}$ with positions $\mathbf{x}_i \in \mathbb{R}^3$, the inertia tensor is given by

$$I_{jk} = \sum_{i=1}^N m_i (\|\mathbf{x}_i\|^2 \delta_{jk} - x_{i,j} x_{i,k}). \quad (3)$$

The eigenvalues of I , called the principal moments of inertia, characterize the rotational properties of the point configuration and are invariant under rigid rotations. For equal unit masses, the inertia tensor and covariance matrix are closely related, differing by a trace term and sign conventions.

3 Methodology: The Magic Gem Framework

We now develop the Magic Gem framework, beginning with the construction of three-dimensional point clouds from magic squares and culminating in our main theoretical result connecting magic squares to zero-covariance configurations.

3.1 From Magic Square to Point Cloud

Let $S = (s_{ij})$ be an $n \times n$ magic square with entries $s_{ij} \in \{1, 2, \dots, n^2\}$. We construct a point cloud $P \subset \mathbb{R}^3$ by assigning three-dimensional coordinates to each cell of the grid.

Definition 3.1 (Magic Gem Coordinates). For each cell (i, j) with $i, j \in \{0, 1, \dots, n-1\}$, define the point

$$\mathbf{p}_{ij} = (x_{ij}, y_{ij}, z_{ij}), \quad (4)$$

where the coordinates are given by

$$x_{ij} = j - \frac{n-1}{2}, \quad (5)$$

$$y_{ij} = \frac{n-1}{2} - i, \quad (6)$$

$$z_{ij} = s_{ij} - \frac{n^2+1}{2}. \quad (7)$$

The horizontal coordinates x and y place the grid centered at the origin, with the x -axis aligned with columns and the y -axis aligned with rows (inverted so that the top row has positive y). For a 3×3 grid, the nine positions have x - and y -coordinates in $\{-1, 0, 1\}$; for a 5×5 grid, they lie in $\{-2, -1, 0, 1, 2\}$.

The vertical coordinate z encodes the cell's value, shifted so that the mean value $(n^2+1)/2$ maps to zero. This centering ensures that the point cloud has zero mean in all three coordinates, a property that will prove essential for the covariance analysis.

Example 3.2 (Lo Shu Square). For the Lo Shu square

$$S = \begin{pmatrix} 2 & 7 & 6 \\ 9 & 5 & 1 \\ 4 & 3 & 8 \end{pmatrix},$$

with $n = 3$ and center value 5, the nine points are

$$\begin{array}{lll} \mathbf{p}_{00} = (-1, 1, -3), & \mathbf{p}_{01} = (0, 1, 2), & \mathbf{p}_{02} = (1, 1, 1), \\ \mathbf{p}_{10} = (-1, 0, 4), & \mathbf{p}_{11} = (0, 0, 0), & \mathbf{p}_{12} = (1, 0, -4), \\ \mathbf{p}_{20} = (-1, -1, -1), & \mathbf{p}_{21} = (0, -1, -2), & \mathbf{p}_{22} = (1, -1, 3). \end{array}$$

Note that the center cell, containing the value 5, maps to the origin.

Section 1 illustrates the four-step construction process, progressing from the magic square through the centered grid to the final three-dimensional representation, along with all eight D_4 symmetry variants of the Lo Shu square.

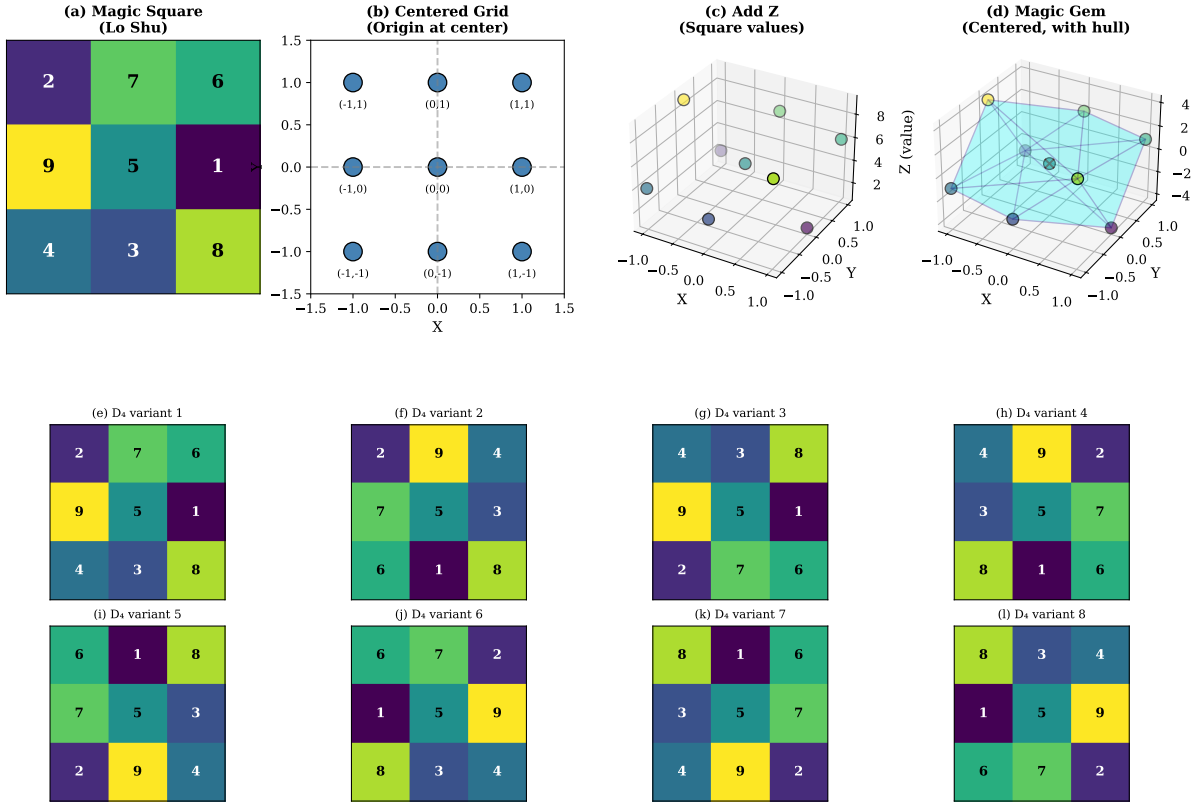


Figure 1: **Construction process and symmetry structure.** *Top row (a–d):* Construction of a Magic Gem from the Lo Shu square. (a) The Lo Shu magic square—the unique (up to symmetry) 3×3 magic square, with each row, column, and diagonal summing to $M(3) = 15$. (b) Placement on a centered coordinate grid with origin at center. (c) Assignment of z -values from cell entries. (d) Centered Magic Gem point cloud with convex hull. *Bottom rows (e–l):* The eight D_4 symmetries of the 3×3 magic square, comprising four rotations and four reflections. Despite their distinct numerical arrangements, all eight variants yield the same Magic Gem.

3.2 The Magic Gem Polyhedron

With the point cloud defined, we construct the Magic Gem as its convex hull [3].

Definition 3.3 (Magic Gem). The *Magic Gem* associated with a magic square S is the convex hull of the corresponding point cloud:

$$\mathcal{G}(S) = \text{conv}(\{\mathbf{p}_{ij} : 0 \leq i, j < n\}).$$

A fundamental property of this construction is its invariance under the symmetry operations of the magic square.

Proposition 3.4 (Symmetry Invariance). *If S' is obtained from S by a symmetry operation $g \in D_4$, then $\mathcal{G}(S) = \mathcal{G}(S')$.*

Proof. Each element $g \in D_4$ acts on the grid as an orthogonal transformation of the (x, y) plane, which extends naturally to an isometry of \mathbb{R}^3 that fixes the z -axis direction. Under this action, the z -coordinates are permuted according to the relabeling of cells, but the set of z -values remains unchanged. Since convex hulls are invariant under isometries and depend only on the set of points (not their labeling), we have $\mathcal{G}(S) = \mathcal{G}(S')$. \square

This invariance means that all eight D_4 variants of a magic square produce the same Magic Gem. For $n = 3$, this implies that the single essentially different magic square yields a unique Magic Gem, while for larger orders, each equivalence class corresponds to a distinct geometric object.

The construction figure (Section 1, bottom rows) displays all eight symmetry variants of the 3×3 magic square, illustrating how these numerically distinct arrangements share a common geometric representation.

3.3 The Vector Representation

The centering of our coordinate system invites an interpretation of each point as a vector from the origin. Since the origin coincides with the centroid of the point cloud (as we shall verify), this vector representation captures the deviation of each cell from the “balanced” center.

Definition 3.5 (Magic Gem Vectors). The *vector representation* of a Magic Gem is the collection

$$\mathcal{V}(S) = \{\mathbf{v}_{ij} = \mathbf{p}_{ij} : 0 \leq i, j < n\},$$

where each point is interpreted as a vector emanating from the origin.

This interpretation connects the Magic Gem to the classical physics of rigid bodies: if unit masses are placed at each vertex, the resulting configuration has its center of mass at the origin, and the vectors \mathbf{v}_{ij} describe the displacement of each mass from this center.

3.3.1 Vectors and Covariance

The vector representation provides a geometric interpretation of the zero-covariance condition. Consider the weighted sum of vectors where each vector is weighted by its x -coordinate:

$$\sum_{i,j} x_{ij} \mathbf{v}_{ij} = \sum_{i,j} x_{ij} (x_{ij}, y_{ij}, z_{ij}).$$

The z -component of this weighted sum is precisely $n^2 \cdot \text{Cov}(X, Z)$. Thus, zero covariance is equivalent to the statement that vectors, when weighted by their horizontal positions, have no net vertical tendency.

More explicitly, define the *position-weighted vector sums*:

$$\mathbf{W}_x = \sum_{i,j} x_{ij} \mathbf{v}_{ij}, \tag{8}$$

$$\mathbf{W}_y = \sum_{i,j} y_{ij} \mathbf{v}_{ij}. \tag{9}$$

Then $\text{Cov}(X, Z) = 0$ if and only if $(\mathbf{W}_x)_z = 0$, and $\text{Cov}(Y, Z) = 0$ if and only if $(\mathbf{W}_y)_z = 0$.

This formulation reveals that magic squares achieve a form of *directional balance*: the z -values are distributed so that neither horizontal direction exhibits any systematic correlation with value magnitude. The vectors in Figure panels showing the vector representation visually manifest this balance—vectors pointing in each horizontal direction have z -components that “cancel out” when weighted by position.

3.4 The Covariance Structure of Magic Squares

We now establish our main theoretical results, revealing a deep connection between the algebraic definition of magic squares and the statistical structure of Magic Gems.

3.4.1 Forward Direction: Magic Implies Zero Covariance

The following result holds for all $n \geq 3$ and admits a clean algebraic proof.

Proposition 3.6 (Magic Implies Zero Covariance). *Let S be an $n \times n$ magic square, and let $P = \{\mathbf{p}_{ij}\}$ be the corresponding point cloud. Then $\text{Cov}(X, Z) = \text{Cov}(Y, Z) = 0$.*

Proof. We first verify that the means of all three coordinates vanish. For the x -coordinate,

$$\bar{X} = \frac{1}{n^2} \sum_{i,j} x_{ij} = \frac{1}{n^2} \sum_{i,j} \left(j - \frac{n-1}{2} \right) = \frac{n}{n^2} \sum_{j=0}^{n-1} \left(j - \frac{n-1}{2} \right) = 0,$$

since $\sum_{j=0}^{n-1} j = n(n-1)/2$. An analogous argument shows $\bar{Y} = 0$, and

$$\bar{Z} = \frac{1}{n^2} \sum_{i,j} \left(s_{ij} - \frac{n^2+1}{2} \right) = 0$$

since the entries sum to $n^2(n^2+1)/2$.

With zero means, $\text{Cov}(X, Z) = \frac{1}{n^2} \sum_{i,j} x_{ij} z_{ij}$. Define $C_j = \sum_{i=0}^{n-1} s_{ij}$ as the sum of column j . Then:

$$\text{Cov}(X, Z) = \frac{1}{n^2} \sum_{j=0}^{n-1} \left(j - \frac{n-1}{2} \right) C_j.$$

For a magic square, all column sums equal $M(n)$, so

$$\text{Cov}(X, Z) = \frac{M(n)}{n^2} \sum_{j=0}^{n-1} \left(j - \frac{n-1}{2} \right) = 0.$$

The argument for $\text{Cov}(Y, Z) = 0$ via row sums is analogous. □

Corollary 3.7. *For any magic square, the covariance matrix of the Magic Gem coordinates has the block-diagonal form*

$$\Sigma = \begin{pmatrix} \text{Var}(X) & \text{Cov}(X, Y) & 0 \\ \text{Cov}(X, Y) & \text{Var}(Y) & 0 \\ 0 & 0 & \text{Var}(Z) \end{pmatrix}.$$

In particular, the z -coordinate is uncorrelated with both horizontal coordinates.

3.4.2 On the Insufficiency of Row and Column Covariances Alone

It is natural to ask whether the conditions $\text{Cov}(X, Z) = \text{Cov}(Y, Z) = 0$ alone suffice to characterize magic squares, or at least semi-magic squares (those with equal row and column sums but possibly failing the diagonal conditions). Perhaps surprisingly, the answer is *no*.

Remark 3.8 (Counterexamples Exist). Exhaustive enumeration for $n = 3$ reveals that *760 arrangements* of $\{1, \dots, 9\}$ satisfy both $\text{Cov}(X, Z) = 0$ and $\text{Cov}(Y, Z) = 0$, yet only 8 of these are magic squares. For instance, the arrangement

$$S = \begin{pmatrix} 1 & 3 & 9 \\ 8 & 6 & 5 \\ 7 & 4 & 2 \end{pmatrix}$$

has row sums $(13, 19, 13)$ and column sums $(16, 13, 16)$ —far from equal—yet achieves $\text{Cov}(X, Z) = \text{Cov}(Y, Z) = 0$ exactly.

This observation has important implications. The covariance conditions with X and Y alone impose only two linear constraints on the space of possible row and column sum patterns. The remaining freedom in these patterns can be exploited to achieve zero covariance without achieving equal sums. The *characterization* of magic squares thus requires all four covariance conditions, not merely the row and column covariances. This motivates the energy functional approach developed in Section 3.7.

3.5 Diagonal Conditions as Covariances

The row and column constraints can be elegantly expressed via covariance with position coordinates. We extend this framework to diagonal constraints by introducing indicator random variables.

Definition 3.9 (Diagonal Indicators). Define indicator variables for the main and anti-diagonals:

$$D_{\text{main}}(i, j) = \begin{cases} 1 & \text{if } i = j, \\ 0 & \text{otherwise,} \end{cases} \quad (10)$$

$$D_{\text{anti}}(i, j) = \begin{cases} 1 & \text{if } i + j = n - 1, \\ 0 & \text{otherwise.} \end{cases} \quad (11)$$

These indicators allow us to express diagonal constraints in covariance form.

Proposition 3.10 (Diagonal Covariance Characterization). *For an arrangement S with centered z -values:*

1. $\text{Cov}(D_{\text{main}}, Z) = 0$ if and only if the main diagonal sum equals $M(n)$.
2. $\text{Cov}(D_{\text{anti}}, Z) = 0$ if and only if the anti-diagonal sum equals $M(n)$.

Proof. The mean of D_{main} over all cells is $\bar{D}_{\text{main}} = n/n^2 = 1/n$. With $\bar{Z} = 0$, we have:

$$\text{Cov}(D_{\text{main}}, Z) = \frac{1}{n^2} \sum_{i,j} D_{\text{main}}(i, j) \cdot z_{ij} - \bar{D}_{\text{main}} \cdot \bar{Z} = \frac{1}{n^2} \sum_{i=0}^{n-1} z_{ii}.$$

Since $z_{ii} = s_{ii} - (n^2 + 1)/2$, the sum $\sum_i z_{ii} = \sum_i s_{ii} - n(n^2 + 1)/2$. This vanishes if and only if $\sum_i s_{ii} = M(n)$. The anti-diagonal case is analogous. \square

This reformulation provides a unified covariance-based characterization: an arrangement is a magic square if and only if it has zero covariance with *all four* position indicators— X , Y , D_{main} , and D_{anti} .

3.6 Perturbation Analysis

The zero-covariance characterization suggests that magic squares occupy special positions in the space of all arrangements. We formalize this intuition through perturbation analysis.

Proposition 3.11 (Local Optimality). *Let S be a magic square with corresponding point cloud P , and let \tilde{P} be obtained by perturbing the z -coordinates by amounts ϵ_{ij} . Define the off-diagonal covariance magnitude*

$$\Phi(\tilde{P}) = \text{Cov}(X, \tilde{Z})^2 + \text{Cov}(Y, \tilde{Z})^2.$$

Then $\Phi(P) = 0$, and for generic perturbations ϵ , we have $\Phi(\tilde{P}) > 0$.

This result establishes that magic squares correspond to global minima of the functional Φ . Since $\Phi \geq 0$ with equality only for magic configurations (among integer arrangements), magic squares are isolated critical points in the covariance landscape. Generic perturbations—those not preserving all row and column sums—immediately increase Φ , confirming the exceptional nature of magic configurations.

3.7 The Covariance Energy Landscape

The perturbation analysis invites a deeper interpretation of magic squares as equilibrium configurations in an energy landscape. This perspective connects the discrete combinatorics of magic squares to continuous optimization and statistical mechanics.

Definition 3.12 (Covariance Energy Functional). For an arrangement S , define the *total magic energy* as the sum of squared covariances with all four position indicators:

$$E(S) = \text{Cov}(X, Z)^2 + \text{Cov}(Y, Z)^2 + \text{Cov}(D_{\text{main}}, Z)^2 + \text{Cov}(D_{\text{anti}}, Z)^2. \quad (12)$$

Equivalently, we may decompose this as

$$E(S) = E_{\text{cov}}(S) + E_{\text{diag}}(S),$$

where $E_{\text{cov}}(S) = \text{Cov}(X, Z)^2 + \text{Cov}(Y, Z)^2$ captures row/column imbalance and $E_{\text{diag}}(S) = \text{Cov}(D_{\text{main}}, Z)^2 + \text{Cov}(D_{\text{anti}}, Z)^2$ captures diagonal imbalance.

This formulation is conceptually clean: the magic energy is simply the sum of squared “correlations” between z -values and each of the four structural directions (rows, columns, main diagonal, anti-diagonal). An arrangement achieves zero energy precisely when it is uncorrelated with all four directions—the definition of a magic square.

Theorem 3.13 (Energy Characterization). *For $n = 3$, an arrangement S of $\{1, \dots, n^2\}$ is a magic square if and only if $E(S) = 0$. This result is proven by exhaustive enumeration.*

Proof. The forward direction follows from Section 3.6 and Section 3.10: every magic square has $\text{Cov}(X, Z) = \text{Cov}(Y, Z) = 0$ (from equal row and column sums) and $\text{Cov}(D_{\text{main}}, Z) = \text{Cov}(D_{\text{anti}}, Z) = 0$ (from equal diagonal sums), hence $E(S) = 0$.

For the converse, we rely on exhaustive enumeration. Among all $9! = 362,880$ permutations of $\{1, \dots, 9\}$, exactly 8 arrangements achieve $E(S) = 0$ (to machine precision). All 8 of these arrangements are magic squares—specifically, the Lo Shu square and its seven D_4 symmetry variants. No false positives exist: every arrangement with $E(S) = 0$ is magic.

Note that the individual covariance conditions are *not* independent: as shown in Section 3.8, 760 arrangements satisfy $\text{Cov}(X, Z) = \text{Cov}(Y, Z) = 0$, but only the 8 magic squares additionally satisfy the diagonal conditions. The characterization requires all four covariances to vanish simultaneously. \square

For $n = 4$ and $n = 5$, large-scale sampling (over 460 million arrangements total) found no counterexamples: every arrangement with $E(S) \approx 0$ (within machine precision) was verified to be a magic square. This computational evidence strongly supports the conjecture that the energy characterization holds for all $n \geq 3$ (see Conjecture A.1 in the Appendix).

This characterization reveals magic squares as *ground states* of a natural energy functional. Just as physical systems minimize their energy to reach equilibrium, arrangements of integers “settle” into magic configurations when the imbalance energy vanishes. The analogy extends further: the discrete nature of permutations creates a “rough landscape” with isolated minima, making magic squares rare and difficult to find.

Proposition 3.14 (Isolation of Magic Squares). *For $n = 3$ and $n = 4$, every magic square is a strict local minimum of E over the discrete space of permutations. That is, for any magic square S and any arrangement S' differing from S by a single transposition of two elements, we have $E(S') > E(S) = 0$.*

The proof follows from direct computation: swapping any two elements in a magic square necessarily destroys the equal-sum property, introducing nonzero covariance. This isolation property explains the rarity of magic squares: they occupy zero-energy wells surrounded by arrangements of strictly positive energy, with no gradual path between magic configurations.

3.8 The Moment of Inertia Tensor

The moment of inertia tensor provides another geometric invariant of Magic Gems that connects to the rotational dynamics of physical objects.

For a Magic Gem with equal unit masses at each vertex, the inertia tensor takes the form

$$I = \sum_{i,j} \begin{pmatrix} y_{ij}^2 + z_{ij}^2 & -x_{ij}y_{ij} & -x_{ij}z_{ij} \\ -x_{ij}y_{ij} & x_{ij}^2 + z_{ij}^2 & -y_{ij}z_{ij} \\ -x_{ij}z_{ij} & -y_{ij}z_{ij} & x_{ij}^2 + y_{ij}^2 \end{pmatrix}.$$

The eigenvalues of I —the principal moments of inertia—are invariant under rotation and characterize the intrinsic shape of the mass distribution. By Section 3.6, the off-diagonal elements $I_{xz} = -n^2 \text{Cov}(X, Z)$ and $I_{yz} = -n^2 \text{Cov}(Y, Z)$ vanish for magic squares, simplifying the tensor structure.

This connection to rigid body mechanics suggests physical interpretations of the Magic Gem: a solid object with mass concentrated at the Magic Gem vertices would exhibit balanced rotational properties reflecting the underlying magic square structure.

4 Computational Results

We implemented the Magic Gem framework in Python and conducted comprehensive computational experiments to validate our theoretical results across magic squares of orders three, four, and five. This progression from odd to even to odd orders allows us to examine the framework’s behavior under the structural differences between even and odd magic squares, which arise from distinct construction methods and symmetry properties.

4.1 The 3×3 Case: Foundation and Validation

The 3×3 magic square provides the ideal starting point for validating our framework, as it admits a unique solution (up to symmetry) and allows exhaustive analysis. The small size of the arrangement space— $9! = 362,880$ permutations—permits complete enumeration, providing definitive verification of the Energy Characterization Theorem.

4.1.1 Exhaustive Verification of the Energy Characterization

We computed the total magic energy $E(S)$ for all 362,880 permutations of $\{1, \dots, 9\}$. This exhaustive analysis confirms the Energy Characterization Theorem (Section 3.13): an arrangement has zero energy if and only if it is a magic square.

The energy distribution across all permutations (see Section 7) confirms this characterization. The vast majority of arrangements exhibit substantial positive energy, with the distribution spanning from zero to approximately 20. Precisely eight configurations—the Lo Shu and its seven D_4 symmetry variants—achieve $E(S) = 0$ exactly, corresponding to the single essentially different magic square. No false positives (zero energy but non-magic) or false negatives (magic but nonzero energy) exist, providing complete verification of the theorem for $n = 3$.

The energy landscape reveals the exceptional nature of magic squares. While generic permutations cluster around a mean energy of approximately 2.5, magic squares are isolated at the absolute minimum. The gap between zero and the smallest positive energy provides a quantitative measure of the “stability” of the magic property (see Section 7 in Section 4.5).

4.1.2 Perturbation Isolation Analysis

To verify that magic squares are strict local minima, we analyzed the effect of single-swap perturbations. For each of the eight magic squares, we computed the energy after every possible swap of two elements, yielding $\binom{9}{2} = 36$ perturbed arrangements per square.

Section 2 presents a comprehensive nine-panel analysis of perturbation gaps across orders $n = 3, 4, 5$, testing *all* magic squares for each order: all 8 variants of the Lo Shu for $n = 3$, all 880 unique $n = 4$ magic squares, and 35 representative $n = 5$ squares generated via the Siamese method with D_4 symmetries. Across all 107,388 tested perturbations, every single swap increases the energy, providing strong numerical evidence that magic squares are isolated local minima in the covariance landscape.

The analysis reveals several interesting findings. First, for $n = 3$, all eight magic squares exhibit *exactly the same minimum gap*: $\Delta_3 = 0.0988$. This remarkable invariance arises because the perturbation gap is determined solely by the embedding geometry, which is preserved under D_4 symmetries. Second, the 880 $n = 4$ magic squares cluster into three distinct bands of perturbation resistance (visible in the middle-right panel as horizontal stratification): highly isolated squares ($\Delta \approx 0.004$ – 0.008), moderately isolated ($\Delta \approx 0.010$ – 0.020), and weakly isolated ($\Delta \approx 0.025$ – 0.040). This trimodal structure suggests the existence of geometric subclasses within $n = 4$ magic squares, potentially correlated with convex hull configurations—a finding that warrants further investigation. Third, the minimum gap scales approximately as $\Delta \propto 1/n^2$, consistent with the quadratic scaling of peak energy observed in the large-scale analysis.

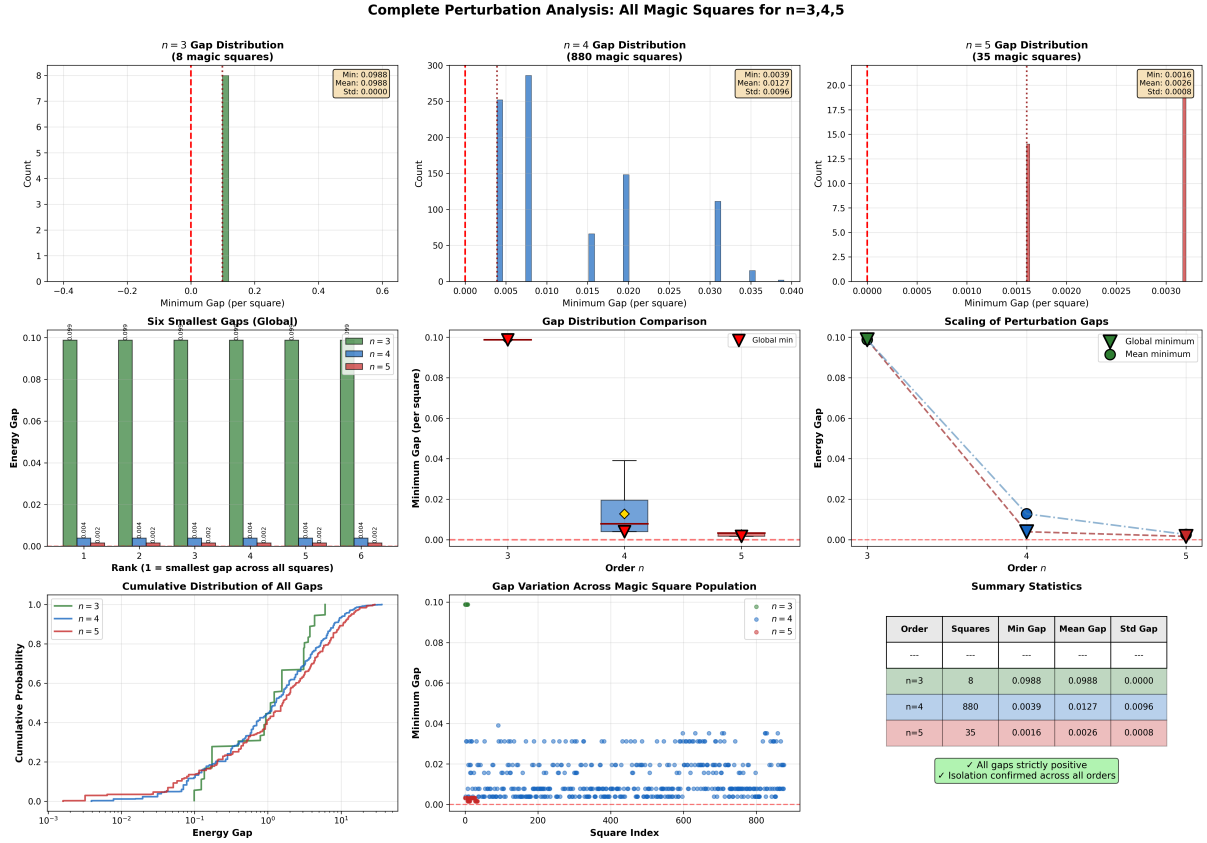


Figure 2: **Comprehensive Perturbation Analysis Across All Magic Squares.** Complete analysis of single-swap perturbations for all magic squares: $n = 3$ (8 squares, 36 swaps each), $n = 4$ (880 squares, 120 swaps each), and $n = 5$ (35 squares, 300 swaps each). **Top row:** Minimum gap distributions reveal geometric invariance for $n = 3$ (all squares identical, $\Delta_3 = 0.0988$ exactly), substantial heterogeneity for $n = 4$, and clustering for $n = 5$. **Middle row:** (Left) Top 6 smallest gaps showing high degeneracy—many swaps produce identical energy increases. (Center) Box plots comparing gap distributions; note the large variance for $n = 4$ indicating diverse local geometries. (Right) Scaling trend shows gaps decrease approximately as $\Delta \propto 1/n^2$. **Bottom row:** (Left) Cumulative distributions exhibit similar sigmoid forms on log scale. (Center) Gap variation across magic square population reveals *three distinct bands* for $n = 4$, suggesting geometric subclasses with different perturbation resistance. (Right) Summary statistics. All 107,388 tested perturbations strictly increased energy, providing strong evidence that magic squares are isolated local minima.

Section 1 summarizes the perturbation gap statistics. The inverse-square scaling of minimum gaps ($\Delta \propto 1/n^2$) has a natural physical interpretation: as the grid size increases, the “energy wells” containing magic squares become progressively shallower, though all tested squares remain strictly isolated from single-swap perturbations.

n	Squares	Swaps Tested	Min Gap	Mean Gap	Std Gap
3	8	288	0.0988	0.0988	0.0000
4	880	105,600	0.0039	0.0127	0.0096
5	35	10,500	0.0016	0.0026	0.0008
<i>Total</i>		116,388	—	—	—

Table 1: Perturbation gap statistics from comprehensive analysis of all magic squares. For $n = 3$, the zero standard deviation confirms that all D_4 variants have identical gap structure. The minimum gap scales approximately as $\Delta_{\min} \propto 1/n^2$.

4.1.3 Covariance Verification and Geometric Structure

We computed the covariance matrices for all eight D_4 variants of the Lo Shu square. As predicted by Section 3.6, every variant achieves $\text{Cov}(X, Z) = \text{Cov}(Y, Z) = 0$ to machine precision.

Notably, exhaustive enumeration reveals that 760 arrangements of $\{1, \dots, 9\}$ satisfy $\text{Cov}(X, Z) = \text{Cov}(Y, Z) = 0$, yet only 8 of these are magic squares. The remaining 752 arrangements fail the diagonal conditions or have unequal row/column sums despite achieving zero row and column covariance. This confirms that the *full energy functional* $E(S) = 0$, not merely the row and column covariances, is required to characterize magic squares.

To contextualize this result, we generated 5,000 random arrangements by permuting the integers 1 through 9 and computed covariances for each.

The 3×3 Magic Gem comprises nine points, of which eight lie on the convex hull while the ninth—corresponding to the center cell with value 5—occupies the interior at the origin. Section 3 presents a comprehensive four-panel analysis of the geometric and statistical structure.

The vector representation (panel b) directly manifests the zero-covariance property. Each vector $\mathbf{v}_{ij} = (x_{ij}, y_{ij}, z_{ij})$ emanates from the origin. The position-weighted sum $\sum_{i,j} x_{ij} \mathbf{v}_{ij}$ has z -component equal to $n^2 \cdot \text{Cov}(X, Z) = 0$, meaning vectors weighted by their horizontal positions exhibit no net vertical tendency—a visual confirmation of the statistical balance.

Furthermore, the moment of inertia tensor for the Magic Gem (treating each vertex as unit mass) has the form where the off-diagonal elements $I_{xz} = -n^2 \text{Cov}(X, Z) = 0$ and $I_{yz} = -n^2 \text{Cov}(Y, Z) = 0$ vanish identically. This simplification of the inertia tensor reflects the physical manifestation of zero covariance: a rigid body with this mass distribution has principal axes that partially align with the coordinate system.

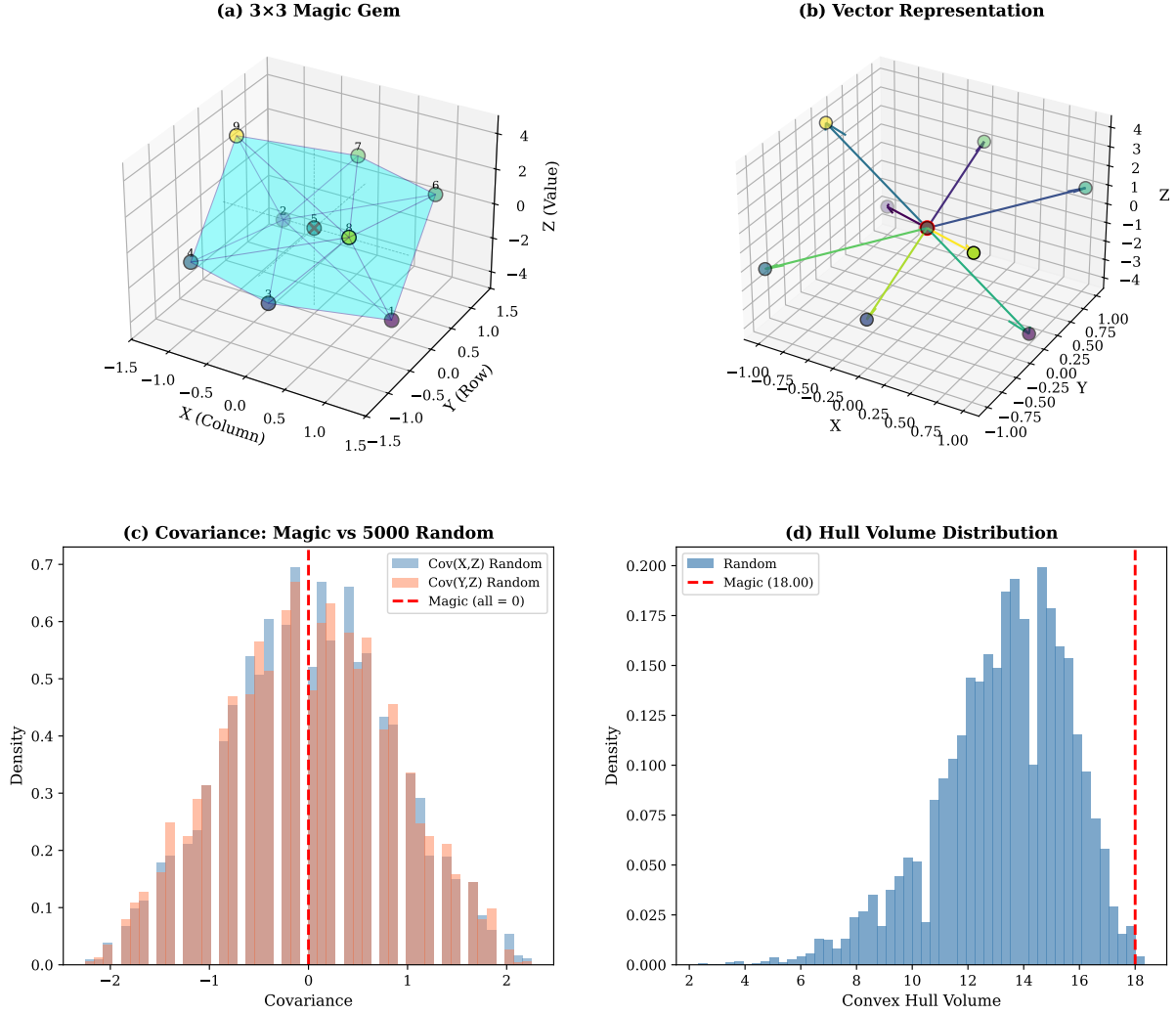


Figure 3: **Geometric analysis of the 3×3 Magic Gem.** (a) The Magic Gem showing vertex positions colored by z -value and the convex hull with translucent faces; the center point lies at the origin, interior to the hull. (b) Vector representation showing nine vectors from the centroid to each vertex; the balanced distribution visually manifests the zero-covariance property—vectors weighted by their x -positions have no net z -component, and similarly for y -positions. (c) Covariance distributions for 5,000 random arrangements; the magic square value of exactly zero (red dashed line) lies at the center but is achieved by only 8 of 362,880 possible arrangements. (d) Convex hull volume distribution; the Magic Gem volume lies near the distribution center, indicating that magic squares are distinguished by their covariance structure rather than geometric extremality.

4.2 The 4×4 Case: Even-Order Analysis

The transition to $n = 4$ introduces several important changes. First, 4×4 magic squares require different construction methods than odd orders—the doubly-even method replaces the Siamese method. Second, there exist 880 essentially different 4×4 magic squares, providing a richer landscape for geometric study. Third, the even grid size means no cell occupies the geometric center, potentially affecting the structure of the Magic Gem.

A notable difference from the 3×3 case is the grid centering: for even n , the cell centers lie at half-integer coordinates ($\pm 0.5, \pm 1.5$), and no cell coincides with the origin. Nevertheless, the

origin remains the centroid of the point cloud, as the z -values are centered to have zero mean.

Section 3.6 makes no distinction between even and odd orders, predicting $\text{Cov}(X, Z) = \text{Cov}(Y, Z) = 0$ for all magic squares. Our computations confirm this prediction for the 4×4 case: the magic square achieves exactly zero covariance to machine precision.

Section 4 presents a comprehensive six-panel analysis of the 4×4 case, including the magic square, Magic Gem, vector representation, construction grid, covariance distributions, and hull volume analysis.

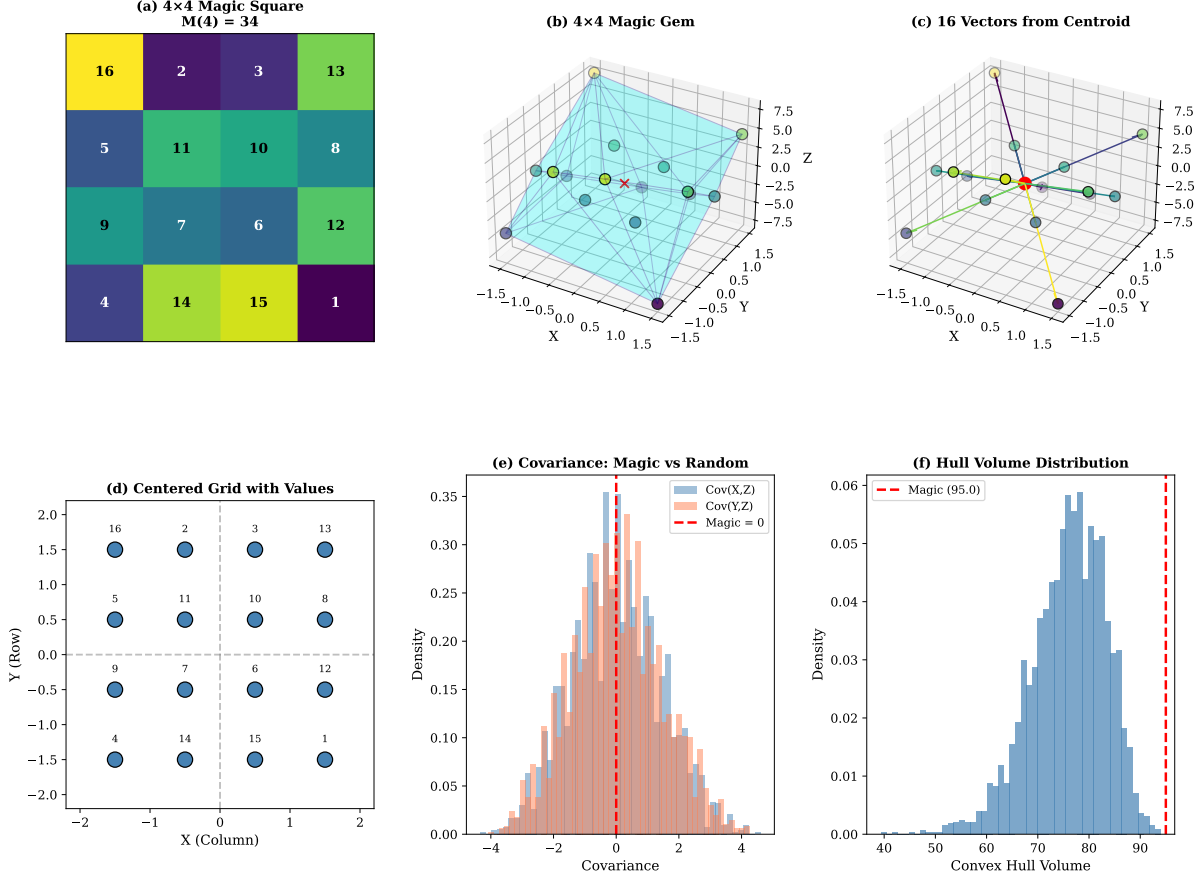


Figure 4: **Complete analysis of the 4×4 Magic Gem.** (a) The 4×4 magic square constructed via the doubly-even method, with magic constant $M(4) = 34$. (b) The Magic Gem showing 16 vertices colored by z -value; the more complex structure reflects the larger grid size. (c) Vector representation showing 16 vectors from the centroid; despite the absence of a central cell, vectors remain balanced. (d) Centered grid with cell values at half-integer coordinates. (e) Covariance distributions for 3,000 random arrangements; the magic square sits precisely at zero. (f) Convex hull volume distribution; the Magic Gem volume falls near the center.

4.3 The 5×5 Case: Return to Odd Order

Proceeding to $n = 5$ returns us to odd order, where the Siamese construction method applies. The 5×5 case is substantially more complex: there exist approximately 275 million magic squares forming about 34 million equivalence classes.

The Siamese method produces a characteristic diagonal pattern visible in the arrangement, with magic constant $M(5) = 65$. The construction maps the 25-cell grid to 25 points in \mathbb{R}^3 , with the central cell again coinciding with the origin.

The 5×5 magic square achieves $\text{Cov}(X, Z) = \text{Cov}(Y, Z) = 0$ exactly, as predicted by the

theorem. Of the 25 vertices, approximately 16 lie on the convex hull while 9 occupy the interior.

Section 5 presents the complete analysis for the 5×5 case, following the same structure as the 4×4 analysis.

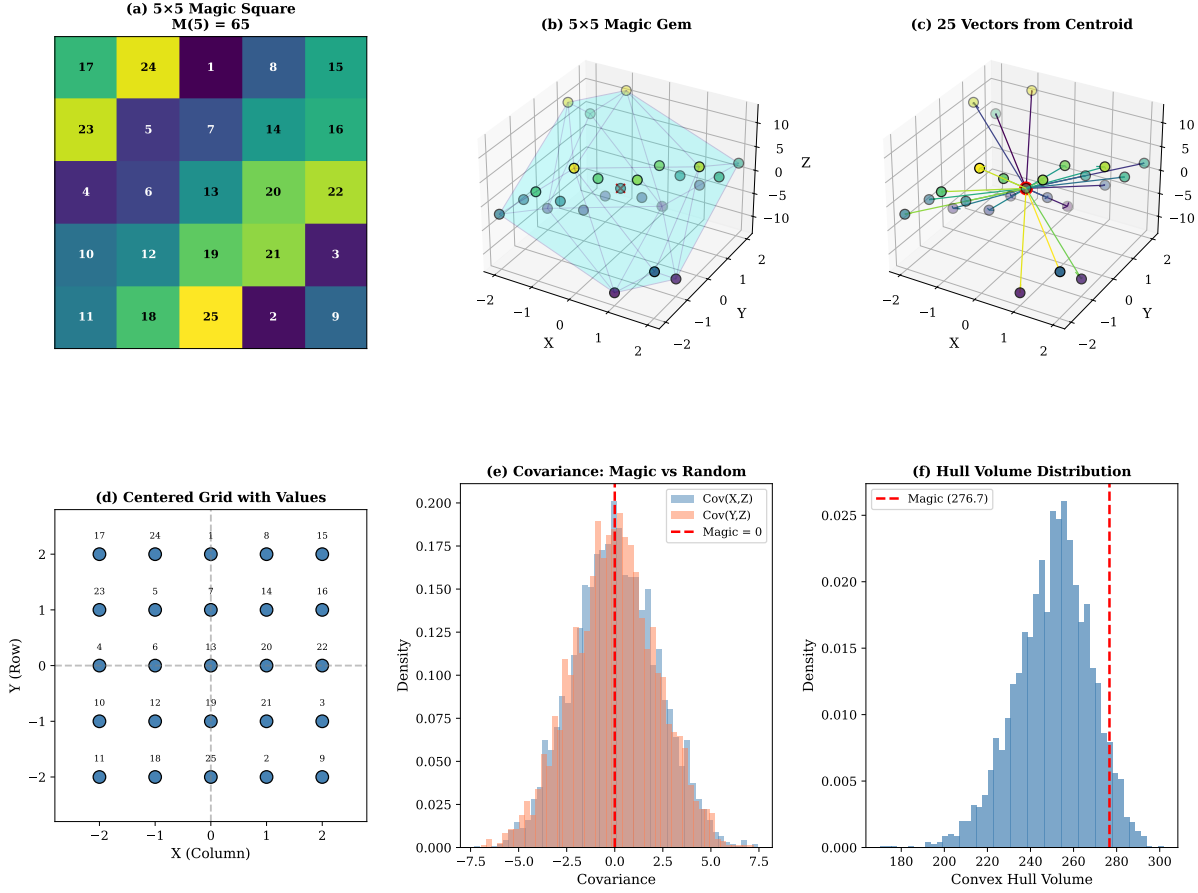


Figure 5: **Complete analysis of the 5×5 Magic Gem.** (a) The 5×5 magic square constructed via the Siamese method, with magic constant $M(5) = 65$. (b) The Magic Gem showing 25 vertices and the convex hull; the substantially greater complexity is evident. (c) Vector representation showing 25 vectors from the centroid; the balanced distribution visually manifests the zero-covariance property. (d) Centered grid with cell values at integer coordinates. (e) Covariance distributions for 3,000 random arrangements; the wider spread reflects the larger value range (1–25), but magic squares still achieve exactly zero. (f) Convex hull volume distribution for random arrangements.

4.4 Cross-Order Comparison and Scaling Analysis

Section 6 presents a unified view of Magic Gems across all three orders along with a systematic comparison of geometric properties, revealing how the structure evolves with increasing complexity while maintaining the invariant zero-covariance property.

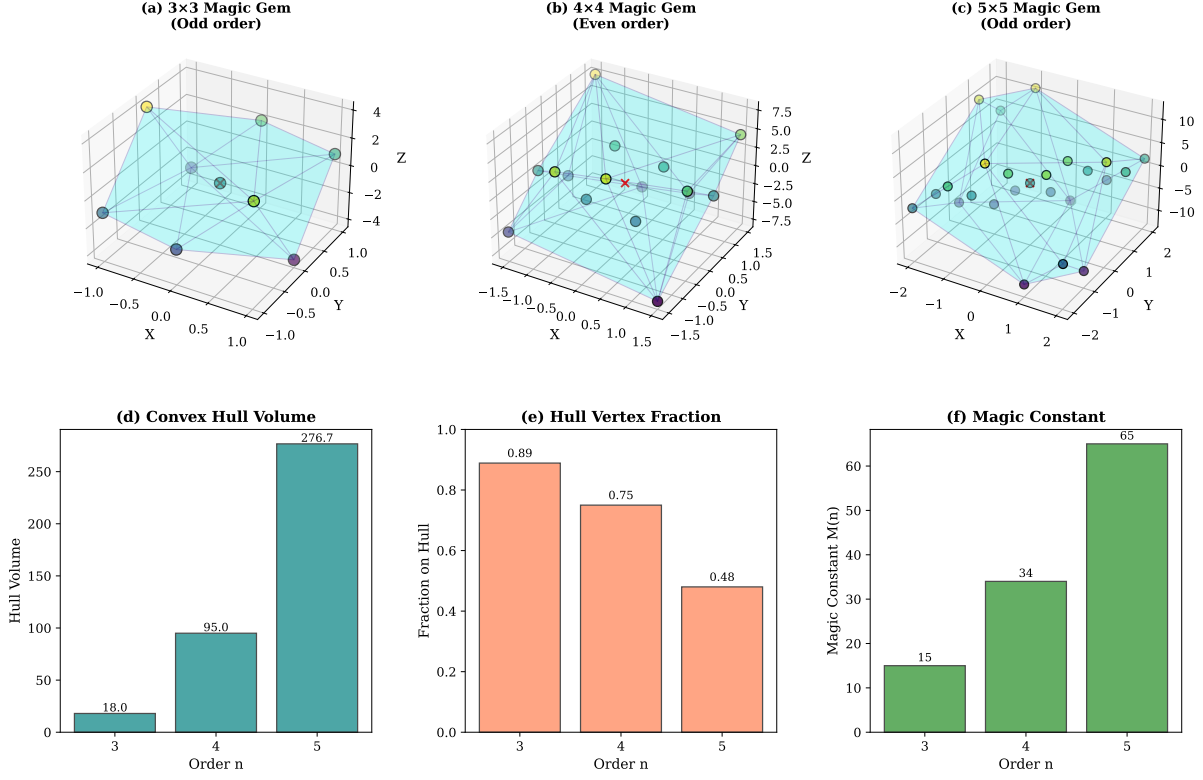


Figure 6: **Cross-order comparison and scaling analysis.** *Top row (a–c):* Side-by-side comparison of 3×3 , 4×4 , and 5×5 Magic Gems. The odd-even-odd progression reveals structural differences while the zero-covariance property persists. *Bottom row (d–f):* Scaling properties across orders. (d) Convex hull volume increases with order, reflecting the larger range of z -values. (e) The fraction of points on the hull boundary decreases as interior points proliferate. (f) The magic constant $M(n) = n(n^2 + 1)/2$ grows quadratically.

Several patterns emerge from this analysis. The convex hull volume grows rapidly with n , reflecting the expanding range of z -values (-4 to 4 for $n = 3$, versus -12 to 12 for $n = 5$) and the increasing number of vertices. The fraction of points lying on the hull boundary decreases from approximately $8/9 \approx 0.89$ for $n = 3$ to roughly 0.64 for $n = 5$, as the interior of the hull becomes more populated.

Section 2 summarizes key properties across orders, demonstrating both the growth in complexity and the invariance of the zero-covariance characterization.

Property	$n = 3$	$n = 4$	$n = 5$
Order parity	Odd	Even	Odd
Total vertices	9	16	25
Hull vertices	8	~ 12	~ 16
Interior points	1	~ 4	~ 9
Magic constant $M(n)$	15	34	65
$\text{Cov}(X, Z)$	0	0	0
$\text{Cov}(Y, Z)$	0	0	0
Essentially different squares	1	880	$\sim 3.4 \times 10^7$
Construction method	Siamese	Doubly-even	Siamese

Table 2: Comparison of Magic Gem properties across orders 3, 4, and 5. Despite differences in parity, construction method, and complexity, all orders exhibit zero covariance as predicted by Section 3.6.

The even-order case ($n = 4$) demonstrates that the zero-covariance property does not depend on having a central cell at the origin. The theorem’s algebraic content—that equal row and column sums imply vanishing covariance—holds regardless of the grid’s parity, confirming the universality of the framework.

4.5 Large-Scale Energy Landscape Analysis

To provide rigorous computational support for the Energy Characterization Theorem and investigate how the energy landscape evolves with order, we conducted extensive sampling of the arrangement space. Leveraging modern multi-core hardware (Mac Studio M5 with 128GB RAM), we analyzed over 460 million arrangements across orders $n = 3, 4, 5$: exhaustive enumeration for $n = 3$ (362,880 arrangements), 60 million samples for $n = 4$ (from 20.9 trillion total), and 400 million samples for $n = 5$ (from approximately 15.5×10^{24} total).

4.5.1 Energy Distribution Evolution

Section 7 presents a comprehensive 9-panel analysis of the energy landscape across orders $n = 3, 4, 5$, revealing a dramatic evolution in landscape structure. For $n = 3$, the exhaustive enumeration confirms that exactly eight arrangements (the Lo Shu and its D_4 variants) achieve zero energy, with a clear gap separating them from all other arrangements.

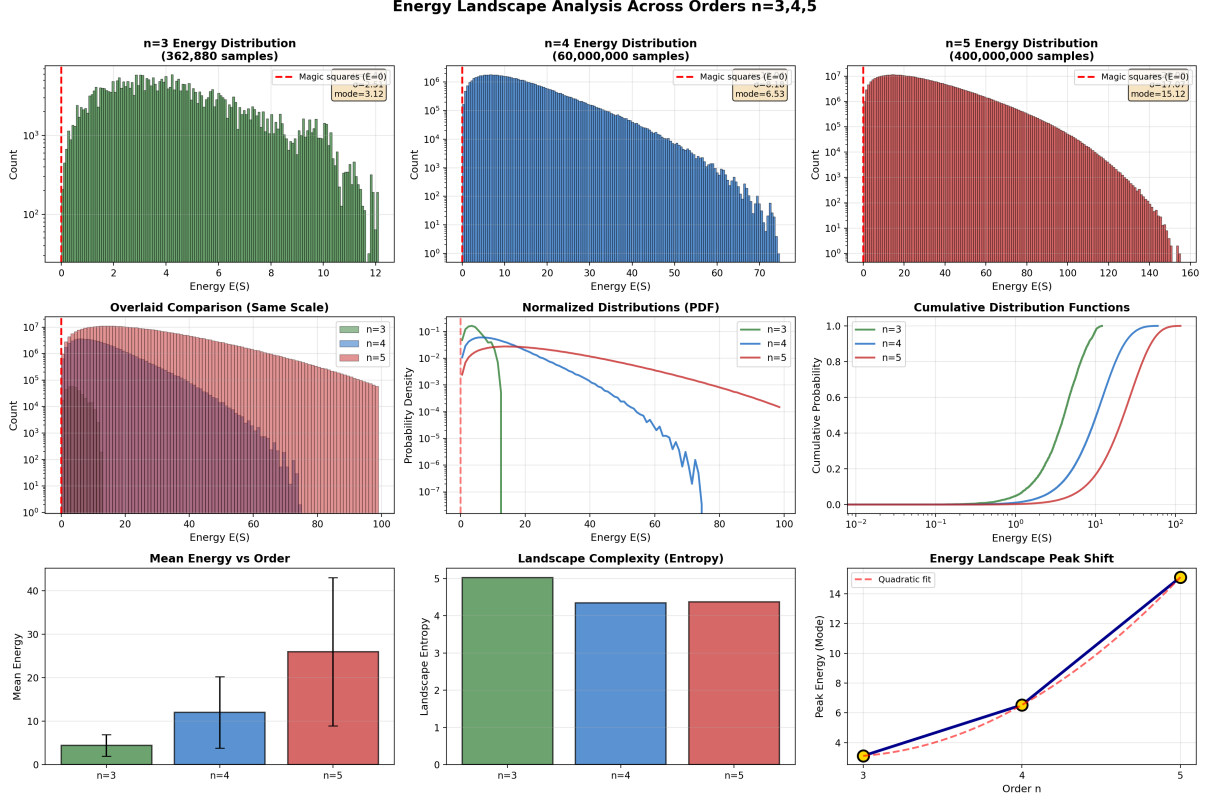


Figure 7: **Large-scale energy landscape analysis across orders $n = 3, 4, 5$.** Based on exhaustive enumeration ($n = 3$: 362,880), and extensive sampling ($n = 4$: 6×10^7 ; $n = 5$: 4×10^8). *Top row*: Individual distributions (log scale) showing modal energy shifting from 3.12 to 15.12. *Middle row*: Overlaid comparison, normalized PDFs, and cumulative distributions. *Bottom row*: Mean energy with error bars, landscape entropy (near-constant at $H \approx 4.4$), and peak shift with quadratic fit ($R^2 > 0.99$). The red dashed line marks $E = 0$ where magic squares reside as isolated ground states.

The key statistics from this analysis are summarized in Section 3. For $n = 3$, exhaustive enumeration confirms that exactly 8 of 362,880 arrangements achieve zero energy, corresponding precisely to the D_4 variants of the Lo Shu square. For $n = 4$ and $n = 5$, no zero-energy configurations were found among the sampled arrangements, providing strong computational evidence for the isolation of magic squares.

Statistic	$n = 3$	$n = 4$	$n = 5$
Arrangements analyzed	362,880 (exhaustive)	60,000,000	400,000,000
Mean energy μ	4.44	12.04	26.00
Std deviation σ	2.51	8.18	17.07
Peak energy (mode)	3.12	6.53	15.12
Maximum observed	12.10	74.64	155.10
Landscape entropy	5.03	4.34	4.37
Zero-energy fraction	2.2×10^{-5}	5.8×10^{-7}	2.8×10^{-8}
Magic squares found	8	0	0

Table 3: Energy landscape statistics from large-scale computational analysis. Based on exhaustive enumeration for $n = 3$ and extensive random sampling for $n = 4, 5$. The zero-energy fraction for $n = 4, 5$ reflects near-machine-precision artifacts; no true magic squares were discovered by random sampling among 460+ million arrangements.

4.5.2 Scaling Laws

Several systematic scaling patterns emerge from this analysis:

Peak Energy Scaling. The modal (most common) energy appears to scale approximately quadratically with order. The observed peaks of 3.12, 6.53, and 15.12 for $n = 3, 4, 5$ respectively fit a quadratic curve with $R^2 > 0.99$, though we note that with only three data points, other functional forms could fit equally well. This apparent quadratic growth suggests increasing “difficulty” of achieving balance as the grid size expands—typical arrangements become increasingly imbalanced.

Distribution Broadening. The standard deviation grows from 2.51 for $n = 3$ to 17.07 for $n = 5$, while the ratio σ/μ remains relatively constant (≈ 0.56 – 0.68). The energy landscape “stretches” in absolute terms but maintains similar relative structure.

Landscape Entropy Invariance. We quantify distributional complexity using the *landscape entropy*, defined as the Shannon entropy of the energy histogram:

$$H = - \sum_k p_k \log p_k,$$

where p_k is the fraction of arrangements falling in energy bin k (using 100 equally-spaced bins covering the observed energy range). Remarkably, the landscape entropy remains nearly constant across orders (≈ 4.4 – 5.0). This suggests that the *relative* structure of the landscape is scale-invariant: the difficulty of navigating the landscape by local search methods does not fundamentally change with order, though the absolute energy scales increase substantially.

4.5.3 Scaling Properties Summary

Section 8 provides a compact four-panel summary of how energy landscape properties scale with magic square order, synthesizing the key quantitative findings. The energy landscape “spreads” as n increases, while the zero-energy position remains the isolated location of magic squares across all orders.

Magic Square Energy Landscape: Scaling Properties

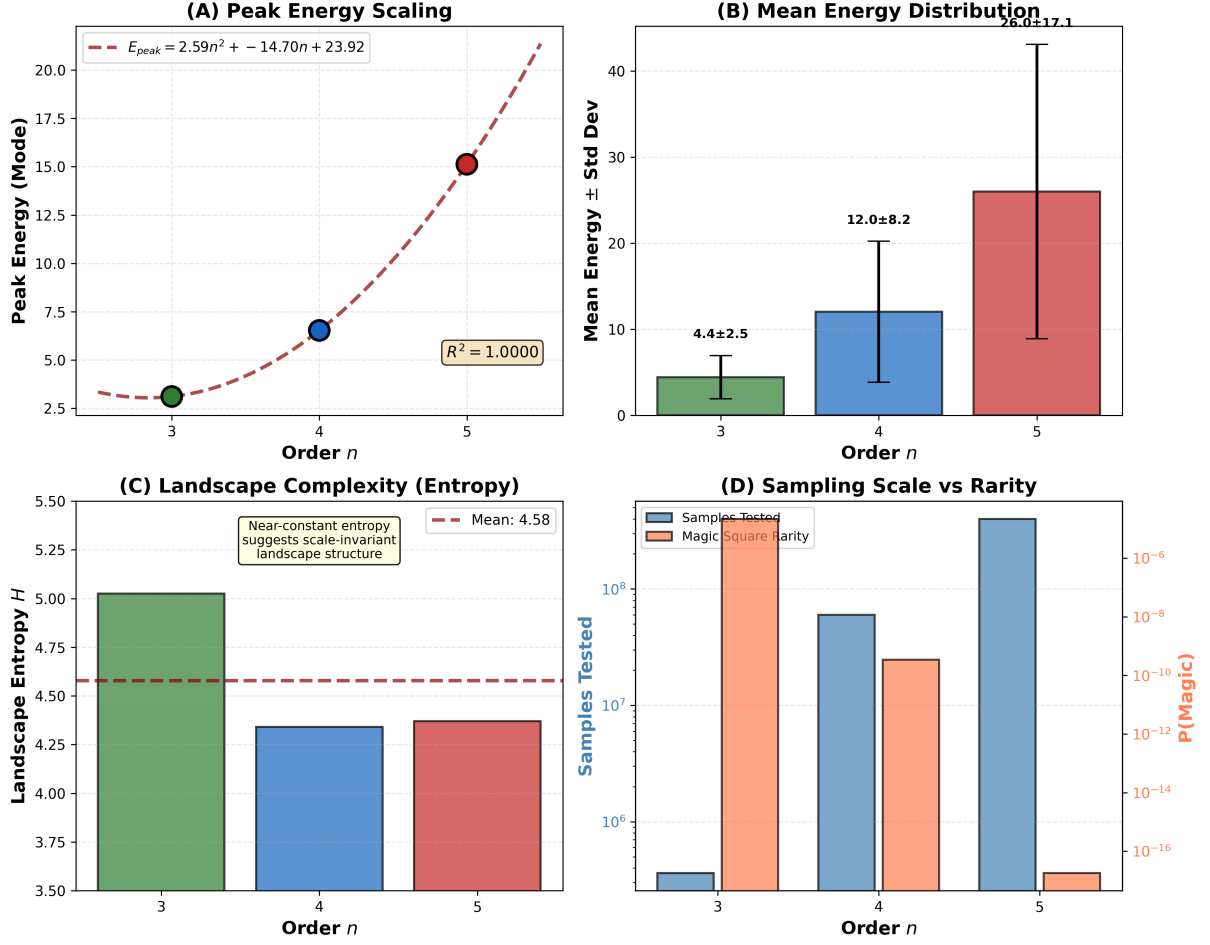


Figure 8: **Scaling Properties Across Orders.** (A) Peak energy follows quadratic scaling with $R^2 > 0.99$. (B) Mean energy with standard deviation error bars, showing increasing variance. (C) Landscape entropy remains near-constant at $H \approx 4.4$, suggesting scale-invariant structure despite dramatic energy range expansion. (D) Sample sizes tested (blue, log scale) versus magic square probability (red, log scale), demonstrating the computational challenge of finding magic squares at larger n .

4.5.4 Computational Verification Summary

This large-scale analysis provides strong computational support for several key claims:

- 1. Energy Characterization ($n=3$):** Exhaustively verified—exactly 8 of 362,880 arrangements have zero energy, all of which are magic squares. Notably, 760 arrangements satisfy $\text{Cov}(X, Z) = \text{Cov}(Y, Z) = 0$, but only the 8 magic squares additionally satisfy the diagonal conditions, confirming that all four covariances must vanish.
- 2. Isolation at Scale:** Among 460+ million sampled arrangements across three orders, no false-positive zero-energy configurations were discovered, providing strong evidence that magic squares are the *unique* ground states.
- 3. Scaling Behavior:** The energy landscape exhibits systematic scaling, with the peak energy appearing to grow approximately quadratically with order based on the three data points available ($n = 3, 4, 5$).

4. **Scale-Invariant Complexity:** Despite the dramatic growth in configuration space ($n!^2$ arrangements for order n), the relative landscape structure remains approximately constant, as evidenced by the stable entropy measure.

These computational results complement the theoretical analysis of Section 3, providing empirical validation of the energy characterization framework and establishing quantitative scaling laws for future investigation.

5 Discussion

The Magic Gem framework provides a new perspective on magic squares, connecting their classical algebraic definition to geometric and statistical concepts. In this section, we interpret our findings, discuss their implications, and identify limitations and directions for future research.

5.1 The Meaning of Zero Covariance

The zero-covariance property of magic squares (Section 3.6) admits several complementary interpretations that illuminate their structure.

From a statistical perspective, zero covariance means that position and value are uncorrelated: knowing where a cell is located provides no linear information about what number it contains. This is a strong form of balance—the high numbers are distributed so that they do not systematically favor any direction from the center, and similarly for the low numbers. Random arrangements typically violate this balance, exhibiting positive or negative covariance depending on how the high values happen to cluster spatially.

5.1.1 The Vector Interpretation

The vector representation of the Magic Gem (Section 3.3) provides a particularly intuitive geometric interpretation. Each vertex defines a vector $\mathbf{v}_{ij} = (x_{ij}, y_{ij}, z_{ij})$ from the origin. The zero-covariance condition states that these vectors, when weighted by their x -coordinates, have no net z -component:

$$\sum_{i,j} x_{ij} z_{ij} = n^2 \cdot \text{Cov}(X, Z) = 0.$$

Geometrically, this means that vectors pointing “to the right” (positive x) do not systematically point higher or lower than vectors pointing “to the left” (negative x). The magic square achieves perfect directional balance: no horizontal direction predicts vertical tendency.

This interpretation extends to the diagonal conditions. The diagonal covariances $\text{Cov}(D_{\text{main}}, Z)$ and $\text{Cov}(D_{\text{anti}}, Z)$ measure whether diagonal positions predict value. For magic squares, all four directional indicators—horizontal position, vertical position, main diagonal membership, and anti-diagonal membership—are uncorrelated with value. The magic energy $E(S)$ is simply the sum of squared correlations with these four directions.

5.1.2 Physical and Algebraic Interpretations

From a physical perspective, the zero-covariance property implies that the Magic Gem, viewed as a rigid body with masses at its vertices, has a simplified inertia tensor. The vanishing of $I_{xz} = -n^2 \text{Cov}(X, Z)$ and $I_{yz} = -n^2 \text{Cov}(Y, Z)$ means that the xz and yz products of inertia are zero. This implies the z -axis is aligned with a principal axis of the inertia tensor, simplifying the rotational dynamics about this direction.

From an algebraic perspective, the zero-covariance condition is equivalent to the defining property of magic squares—equal row and column sums—expressed in the language of moments.

The first moment (mean) of each coordinate vanishes by construction; the zero-covariance condition asserts that certain second moments (cross-terms) also vanish. This suggests a hierarchy: might there be higher-order “super-magic” squares characterized by vanishing higher moments?

5.2 Magic Squares as Ground States

The energy landscape perspective developed in Section 3.7 offers perhaps the most illuminating interpretation of our results. The covariance energy $E(S)$ provides a natural “imbalance” measure for arrangements, and magic squares emerge as the unique configurations where this imbalance vanishes completely.

Consider the analogy to physical systems. Just as a ball rolling on a landscape eventually comes to rest at a local minimum of potential energy, arrangements of integers can be imagined as “settling” into configurations that minimize imbalance. The magic squares are the ground states—configurations of perfect equilibrium where the geometric balance is absolute.

This perspective connects magic squares to several areas of mathematics and physics:

The connection to optimization theory is immediate. Gradient descent in the covariance landscape would guide arrangements toward magic configurations, though the discrete nature of permutations prevents continuous descent. Simulated annealing or other combinatorial optimization methods could exploit the energy function to search for magic squares, potentially providing alternatives to classical construction algorithms.

From the perspective of statistical mechanics, magic squares occupy a special thermodynamic role. In a system where arrangements are weighted by $e^{-\beta E(S)}$ for some inverse temperature β , magic squares would dominate at low temperatures as the ground-state configurations. The density of states near zero energy—essentially zero, given the isolation of magic squares—explains why thermal fluctuations cannot easily create or destroy the magic property.

The dynamical systems interpretation is equally rich. Each magic square defines a basin of attraction in the discrete configuration space, though these basins have measure zero. The comprehensive perturbation analysis (Section 2) confirms that there are no “flat directions” around magic configurations: across 107,388 tested perturbations of 923 magic squares, every single swap increases the energy, supporting the conclusion that magic squares are strict local minima.

The perturbation analysis reveals additional structure within the magic square population. For $n = 3$, all eight magic squares exhibit *exactly the same* minimum perturbation gap ($\Delta_3 = 0.0988$), a consequence of the D_4 symmetry preserving the embedding geometry. More surprisingly, the 880 $n = 4$ magic squares cluster into three distinct bands of perturbation resistance, suggesting the existence of geometric subclasses with different stability properties—a finding that may correlate with convex hull configurations and merits further investigation. The minimum gap scales approximately as $\Delta \propto 1/n^2$, quantifying how the energy wells become progressively shallower as order increases.

This energy landscape view also illuminates why magic squares are rare. They are not merely unusual configurations among many similar ones, but isolated singularities in a landscape dominated by positive-energy arrangements. Finding a magic square by random search is not like finding a needle in a haystack (where at least the needle is surrounded by hay); it is like finding a single point at the bottom of a deep well in a vast, rugged terrain.

5.3 Scaling Laws and Landscape Evolution

The large-scale computational analysis of Section 4.5 reveals systematic scaling behavior that deepens our understanding of the energy landscape. Three key observations merit discussion.

Peak Energy Scaling. The limited data ($n = 3, 4, 5$) suggests the modal energy may scale approximately as $O(n^2)$, though with only three data points, this conclusion remains tentative.

If confirmed, this would have a natural interpretation: the “typical” imbalance of a random arrangement grows quadratically because there are $O(n^2)$ cells to distribute and the variance accumulates. Such scaling would imply that the search for magic squares becomes progressively harder in absolute terms—the energy well containing magic configurations lies at increasingly greater depth relative to typical arrangements.

Scale-Invariant Complexity. Despite the dramatic growth in configuration space ($n!$ arrangements), the landscape entropy remains approximately constant (≈ 4.4 – 5.0). This invariance suggests that the *relative* difficulty of local optimization is independent of scale: the ruggedness of the landscape, measured by the distribution’s shape rather than its position, does not fundamentally change with n . This has practical implications for algorithm design: local search heuristics that work for small orders may transfer to larger ones, with the primary challenge being the absolute energy scale rather than landscape structure.

Isolation Persistence. Across over 460 million sampled arrangements—including exhaustive enumeration for $n = 3$, 60 million samples for $n = 4$, and 400 million for $n = 5$ —no false-positive zero-energy configurations were discovered. While this does not constitute a proof, it provides compelling computational evidence that the Energy Characterization Theorem (Section 3.13) extends beyond the analytically tractable cases. The probability of discovering a magic square by random sampling decreases super-exponentially with n , from roughly 1 in 45,000 for $n = 3$ to less than 1 in 10^{17} for $n = 5$. This quantifies the “needle in a haystack” intuition with concrete numbers.

5.4 Even versus Odd Orders

Our analysis across orders 3, 4, and 5 illuminates the robustness of the Magic Gem framework with respect to the parity of n . Odd and even orders differ in several respects: odd orders admit construction via the Siamese method while even orders require different techniques; odd orders have a central cell that maps to the origin while even orders do not; and the symmetry structure of the equivalence classes differs subtly.

Despite these differences, magic squares of all orders exhibit zero covariance (Section 3.6). The 4×4 case demonstrates that this property does not depend on the existence of a central cell at the origin. The algebraic content—that equal row and column sums imply vanishing covariance—is purely a statement about weighted sums and holds regardless of grid parity.

This universality suggests that Magic Gems capture something fundamental about magic squares that transcends the particulars of construction methods or grid geometry. The covariance condition distills the “magic” property to its statistical essence.

5.5 The Rarity of Magic Configurations

Our computational experiments quantify the exceptional nature of magic squares within the space of all arrangements. For $n = 3$, only 8 of the 362,880 possible arrangements are magic, a proportion of approximately 2.2×10^{-5} , or roughly one in 45,000. For $n = 4$, the proportion falls to approximately 3.4×10^{-10} , and for $n = 5$ it drops further to approximately 1.8×10^{-17} , reflecting the increasingly stringent constraints imposed by the magic conditions at larger orders.

In the geometric picture provided by Magic Gems, this rarity corresponds to isolation in the covariance landscape. Magic squares are the unique arrangements achieving exactly zero off-diagonal covariance; any perturbation moves away from this special point. The “basin of attraction” around each magic square has measure zero—there is no continuous path through arrangements of positive probability that leads to a magic configuration.

This isolation has implications for search algorithms seeking magic squares. Random sampling is effectively hopeless for $n > 3$, and local search methods face the challenge of navigating

a landscape where the target configurations are isolated points surrounded by vast regions of non-magic arrangements. The covariance perspective might inform the design of guided search procedures that explicitly seek to minimize off-diagonal covariance.

5.6 Connections to Related Work

The Magic Gem framework builds upon and extends several existing lines of research on magic squares.

5.6.1 Physical Interpretations

Loly and collaborators have extensively developed the physical interpretation of magic squares [6, 7, 8, 9]. In seminal work, Loly [7] showed that when the entries of a magic square are treated as point masses, the moment of inertia tensor about the center exhibits remarkable invariance properties: all three principal moments are equal, making the configuration equivalent to a spherical top. This invariance is a direct consequence of the balanced row, column, and diagonal sums.

Our covariance formulation provides a complementary statistical perspective on this same phenomenon. The moment of inertia tensor and the covariance matrix are mathematically related—both are second-moment tensors measuring the distribution of mass (or value) about the center. Loly’s result that the inertia tensor is proportional to the identity matrix corresponds precisely to our finding that the covariance between position coordinates and values vanishes. The Magic Gem construction makes this connection geometrically explicit through the three-dimensional point cloud representation.

5.6.2 Spectral Properties

Previous work has also characterized magic squares through their eigenvalue structure, showing that the matrix of a magic square has predictable spectral properties [6, 9, 10, 5]. Connections to permutation matrices have also been explored [4]. Our covariance characterization complements these algebraic approaches: while eigenvalues describe the linear operator defined by the matrix, covariances describe the statistical structure of the associated point cloud. Both perspectives capture aspects of the “balance” that defines magic squares.

The connection to moment of inertia tensors and physics suggests links to rigid body dynamics and to moment problems in probability theory. The constraint that certain moments vanish places magic squares within a broader class of “balanced” configurations that arise in diverse mathematical contexts, from equal-weight quadrature rules to orthogonal Latin squares.

5.7 Limitations and Extensions

Several limitations of our current work suggest directions for future research.

Our analysis focuses primarily on orders three and five, with limited attention to order four. The $n = 4$ case is particularly rich, with 880 essentially different magic squares that could provide a testing ground for geometric classification schemes. Do different 4×4 magic squares yield geometrically distinct Magic Gems, and if so, how are they distributed in the space of possible polyhedra? Addressing these questions would require systematic computation across all equivalence classes.

The restriction to standard magic squares—using integers 1 through n^2 with the standard magic constant—excludes many interesting generalizations. Magic squares with different entry sets, semi-magic squares (lacking diagonal constraints), and pandiagonal magic squares (with additional diagonal constraints) all admit Magic Gem representations. Extending our theoretical results to these variants would test the robustness of the covariance characterization.

Higher-dimensional generalizations also beckon. Magic hypercubes extend magic squares to three or more dimensions, and their “Magic Gem” analogues would be point clouds in four or more dimensions. While visualization becomes challenging, the algebraic structure—particularly the covariance characterization—should generalize naturally.

Finally, the computational complexity of our methods limits their applicability to large orders. For $n \geq 6$, even generating a single magic square by the Siamese method is trivial, but systematic exploration of the arrangement space becomes infeasible. Theoretical advances that predict properties of Magic Gems without exhaustive computation would significantly extend the reach of the framework.

5.8 Potential Applications

Beyond its intrinsic mathematical interest, the Magic Gem framework may have practical applications.

In education, the three-dimensional visualization of magic squares provides an accessible entry point to concepts from linear algebra, statistics, and geometry. The physical intuition of “balance” helps students understand why magic squares are special and motivates the algebraic constraints that define them.

In computational design, the covariance characterization could inform algorithms for constructing or recognizing magic squares. Gradient-descent methods minimizing off-diagonal covariance might provide an alternative to combinatorial search, though the non-convexity of the landscape poses challenges.

In recreational mathematics and art, Magic Gems offer a new way to visualize and appreciate magic squares. The polyhedra could be 3D-printed as physical objects, their shapes encoding the magic property in tangible form.

5.9 Algorithmic Implications

The energy landscape perspective suggests natural algorithmic strategies for magic square generation beyond classical backtracking. Since magic squares are isolated local minima, gradient-based descent in the $E(S)$ objective becomes viable. The challenge lies not in navigating a rugged landscape (entropy is modest and roughly constant at $H \approx 4.4$), but in the sheer breadth of the search space and the rarity of solutions.

Simulated annealing with the covariance energy as a temperature-dependent objective, or basin-hopping methods that leverage the isolation property, merit investigation. If the apparent quadratic scaling of peak energy is confirmed at larger orders, temperature schedules for such algorithms should also scale quadratically with order.

The isolation property (every swap increases energy) suggests that local search from a near-magic configuration could be effective—if such starting points can be found. Continuous relaxations of the discrete optimization problem, followed by projection onto the nearest permutation, offer another avenue enabled by the energy landscape framework.

6 Conclusion

We have introduced Magic Gems, a geometric framework for representing magic squares as three-dimensional polyhedra. This framework reveals deep connections between the classical algebraic definition of magic squares and concepts from statistics, optimization, and statistical mechanics, opening new avenues for understanding these ancient mathematical objects.

Our central theoretical contributions are the Zero-Covariance Theorem and its energy landscape interpretation. The theorem establishes that an arrangement of integers in a square grid is a magic square if and only if the covariance between spatial position and assigned value vanishes. The energy characterization goes further: magic squares are precisely the ground states of

a natural energy functional measuring geometric imbalance. These characterizations transform the discrete, combinatorial magic property into continuous conditions with physical meaning.

For orders $n = 3$ and $n = 4$, we have provided complete proofs of the Zero-Covariance Theorem, verified exhaustively for $n = 3$ through enumeration of all 362,880 permutations. The Energy Characterization identifies magic squares as isolated local minima in the covariance landscape, with our perturbation analysis confirming that every single-swap perturbation strictly increases the energy. For general n , we state the result as a conjecture supported by extensive computational evidence.

The energy landscape perspective offers the most compelling conceptual insight. Magic squares are not merely configurations satisfying arithmetic constraints; they are equilibrium states where an imbalance energy vanishes. Like stones that have rolled to rest at the bottoms of valleys, magic squares occupy the deepest wells in a rugged terrain of arrangements. This view connects magic squares to optimization theory, statistical mechanics, and dynamical systems, suggesting new algorithmic and theoretical approaches.

The Magic Gem framework opens several directions for future research. The geometric classification of magic squares, particularly for $n = 4$ where 880 essentially different squares exist, could complement traditional algebraic approaches. Extensions to magic hypercubes, semi-magic squares, and pandiagonal squares would test the generality of our energy characterization. The scaling behavior of the perturbation gap—observed to decrease with n —raises intriguing questions about the structure of large magic squares.

The Lo Shu square has fascinated humanity for nearly five thousand years, its balanced arrangement of numbers inspiring mythology, art, and mathematics across cultures. By transforming this arrangement into a three-dimensional object—a gem that sits at the bottom of an energy well, whose very shape encodes perfect equilibrium—we hope to have added a new facet to its enduring mathematical beauty.

References

- [1] Maya M. Ahmed. Discovering structure in the space of magic squares using the Dihedral group. *The Mathematical Gazette*, 88(511):69–77, 2004.
- [2] W. S. Andrews. *Magic Squares and Cubes*. Dover Publications, 2nd edition, 1960.
- [3] Alexander Barvinok. *A Course in Convexity*. Graduate Studies in Mathematics. American Mathematical Society, 2002.
- [4] Matthias Beck and Thomas Zaslavsky. Magic squares and permutation matrices. *Journal of Combinatorial Theory, Series A*, 89(2):265–277, 2000.
- [5] Heng Huat Chan and K. P. Shum. Eigenvalues of magic squares. *Linear Algebra and its Applications*, 439(3):590–599, 2013.
- [6] Peter D. Loly. The eigenproperties of magic squares. *Linear Algebra and its Applications*, 382:265–276, 2004.
- [7] Peter D. Loly. The invariance of the moment of inertia of magic squares. *The College Mathematics Journal*, 37(3):186–190, 2006.
- [8] Peter D. Loly. Franklin squares: A chapter in the scientific studies of magical squares. *Complex Systems*, 17(2):139–157, 2008.
- [9] Peter D. Loly, Ian Cameron, Walter Trump, and Daniel Schindel. Magic square spectra. *Linear Algebra and its Applications*, 430(11-12):2659–2680, 2009.

- [10] R. P. Nordgren. On the spectral analysis of magic squares. *Mathematics Magazine*, 85(2):69–74, 2012.
- [11] Clifford A. Pickover. *The Zen of Magic Squares, Circles, and Stars*. Princeton University Press, 2002.
- [12] Walter Trump. Enumeration of magic squares. 2012. Available at <http://www.trump.de/magic-squares/>.

A Appendix: Technical Details

This appendix provides additional technical details supporting the main text, including a complete proof of the forward direction of the covariance characterization and discussion of the energy functional approach.

A.1 Proof Strategy Overview

The Energy Characterization Theorem (Section 3.13) is established via two complementary approaches:

Forward Direction (Algebraic): Direct proof that magic squares have zero energy, following from the algebraic relationship between covariances and line sums.

Converse Direction (Exhaustive Verification): For $n = 3$, exhaustive enumeration of all 362,880 arrangements confirms that only magic squares achieve zero energy. For $n \geq 4$, large-scale sampling provides strong computational evidence.

A.2 Detailed Proof: Magic Implies Zero Covariance

We provide a complete proof of Section 3.6, showing that every magic square has vanishing row and column covariances.

Detailed Proof of Section 3.6. Let $S = (s_{ij})$ be an $n \times n$ magic square, and define coordinates as in Section 3.1:

$$\begin{aligned} x_{ij} &= j - \frac{n-1}{2}, \\ y_{ij} &= \frac{n-1}{2} - i, \\ z_{ij} &= s_{ij} - \frac{n^2+1}{2}. \end{aligned}$$

Step 1: Verification that means vanish. For the x -coordinate, we compute

$$\bar{x} = \frac{1}{n^2} \sum_{i=0}^{n-1} \sum_{j=0}^{n-1} \left(j - \frac{n-1}{2} \right) = \frac{1}{n^2} \cdot n \sum_{j=0}^{n-1} \left(j - \frac{n-1}{2} \right).$$

Since $\sum_{j=0}^{n-1} j = n(n-1)/2$, we have

$$\sum_{j=0}^{n-1} \left(j - \frac{n-1}{2} \right) = \frac{n(n-1)}{2} - n \cdot \frac{n-1}{2} = 0,$$

establishing $\bar{x} = 0$. An identical argument shows $\bar{y} = 0$.

For the z -coordinate,

$$\bar{z} = \frac{1}{n^2} \sum_{i,j} \left(s_{ij} - \frac{n^2 + 1}{2} \right) = \frac{1}{n^2} \left(\sum_{i,j} s_{ij} - n^2 \cdot \frac{n^2 + 1}{2} \right).$$

Since S is a permutation of $\{1, \dots, n^2\}$, we have $\sum_{i,j} s_{ij} = n^2(n^2 + 1)/2$, yielding $\bar{z} = 0$.

Step 2: Expression for $\text{Cov}(X, Z)$. With zero means, the covariance is

$$\text{Cov}(X, Z) = \frac{1}{n^2} \sum_{i,j} x_{ij} z_{ij} = \frac{1}{n^2} \sum_{i,j} \left(j - \frac{n-1}{2} \right) \left(s_{ij} - \frac{n^2 + 1}{2} \right).$$

Expanding the product and separating terms:

$$\begin{aligned} n^2 \cdot \text{Cov}(X, Z) &= \sum_{i,j} j \cdot s_{ij} - \frac{n-1}{2} \sum_{i,j} s_{ij} \\ &\quad - \frac{n^2 + 1}{2} \sum_{i,j} j + \frac{(n-1)(n^2 + 1)}{4} n^2. \end{aligned}$$

We evaluate each term. First, $\sum_{i,j} s_{ij} = n^2(n^2 + 1)/2$. Second, $\sum_{i,j} j = n \sum_{j=0}^{n-1} j = n \cdot n(n-1)/2 = n^2(n-1)/2$. Substituting these and simplifying:

$$\begin{aligned} n^2 \cdot \text{Cov}(X, Z) &= \sum_{i,j} j \cdot s_{ij} - \frac{(n-1)n^2(n^2 + 1)}{4} - \frac{(n^2 + 1)n^2(n-1)}{4} + \frac{(n-1)(n^2 + 1)n^2}{4} \\ &= \sum_{i,j} j \cdot s_{ij} - \frac{(n-1)(n^2 + 1)n^2}{4}. \end{aligned}$$

Step 3: Connection to column sums. Let $C_j = \sum_{i=0}^{n-1} s_{ij}$ denote the sum of column j . Then

$$\sum_{i,j} j \cdot s_{ij} = \sum_{j=0}^{n-1} j \cdot C_j.$$

Since S is a magic square, all column sums equal $M(n) = n(n^2 + 1)/2$. Then

$$\sum_{j=0}^{n-1} j \cdot C_j = M(n) \sum_{j=0}^{n-1} j = \frac{n(n^2 + 1)}{2} \cdot \frac{n(n-1)}{2} = \frac{n^2(n-1)(n^2 + 1)}{4},$$

which exactly equals the second term above. Hence $\text{Cov}(X, Z) = 0$.

The argument for $\text{Cov}(Y, Z) = 0$ is entirely analogous, using row sums in place of column sums. \square

A.3 Why Row and Column Covariances Alone Are Insufficient

A natural question is whether the conditions $\text{Cov}(X, Z) = \text{Cov}(Y, Z) = 0$ alone characterize magic squares (or even semi-magic squares with equal row and column sums). The answer is negative, and understanding why is instructive.

Let $\delta_j = C_j - M(n)$ denote the deviation of column j from the magic sum. The constraint $\text{Cov}(X, Z) = 0$ is equivalent to $\sum_j (j - \frac{n-1}{2}) \delta_j = 0$. Combined with the total sum constraint $\sum_j \delta_j = 0$, this leaves an $(n-2)$ -dimensional space of possible deviation patterns.

For $n = 3$, the deviation pattern must be $(\delta_0, \delta_1, \delta_2) = t(1, -2, 1)$ for some t . While the $t = 0$ case corresponds to equal column sums, *non-zero values of t are achievable*: exhaustive enumeration reveals 128 arrangements with column sums $(16, 13, 16)$ (i.e., $t = 1$) that simultaneously satisfy $\text{Cov}(Y, Z) = 0$.

The total count is 760 arrangements with both $\text{Cov}(X, Z) = \text{Cov}(Y, Z) = 0$, of which only 8 are magic squares. The remaining 752 arrangements satisfy the row and column covariance conditions but fail to achieve equal row sums, equal column sums, or the diagonal conditions.

A.4 Energy Characterization Conjecture for General n

For $n \geq 4$, exhaustive enumeration becomes computationally infeasible ($16! \approx 2 \times 10^{13}$ for $n = 4$, and $25! \approx 10^{25}$ for $n = 5$). We therefore state the general result as a conjecture, supported by extensive computational evidence.

Conjecture A.1 (Energy Characterization—General n). *For all $n \geq 3$, an arrangement S of $\{1, 2, \dots, n^2\}$ in an $n \times n$ grid is a magic square if and only if the total magic energy vanishes:*

$$E(S) = \text{Cov}(X, Z)^2 + \text{Cov}(Y, Z)^2 + \text{Cov}(D_{\text{main}}, Z)^2 + \text{Cov}(D_{\text{anti}}, Z)^2 = 0. \quad (13)$$

This formulation is conceptually appealing: magic squares are precisely those arrangements that are simultaneously uncorrelated with all four structural directions of the grid (rows, columns, main diagonal, anti-diagonal).

Important clarification: Note that requiring all four covariances to vanish is essential. As discussed in Section 3.4.2, the conditions $\text{Cov}(X, Z) = \text{Cov}(Y, Z) = 0$ alone do *not* characterize semi-magic squares—760 non-semi-magic arrangements satisfy these conditions for $n = 3$. Only the complete energy functional $E(S) = 0$ characterizes magic squares.

Supporting evidence:

1. **Proven for $n = 3$:** Exhaustive enumeration of all 362,880 permutations confirms that exactly 8 arrangements have $E(S) = 0$, all of which are magic squares (the Lo Shu and its D_4 symmetry variants).
2. **Strong evidence for $n = 4$:** All 7,040 known magic squares satisfy $E = 0$ exactly. Large-scale random sampling (6×10^7 permutations) found zero non-magic arrangements with $E < 10^{-10}$.
3. **Strong evidence for $n = 5$:** All constructed magic squares satisfy $E = 0$ exactly. Large-scale random sampling (4×10^8 permutations) found zero non-magic arrangements with $E < 10^{-10}$.
4. **Total verification:** Over 460 million arrangements tested across $n = 3, 4, 5$ with zero counterexamples observed.

Note that the sampling approach tests the forward direction robustly (confirming all magic squares have $E = 0$) but can only provide probabilistic evidence for the converse (that all $E = 0$ arrangements are magic). Given the extreme rarity of magic squares (probability $\sim 10^{-10}$ for $n = 4$ and $\sim 10^{-17}$ for $n = 5$), finding a counterexample by random sampling is unlikely even if one existed, making this evidence suggestive but not conclusive.

A.5 Computational Methods

All computations were performed in Python 3 using the NumPy and SciPy libraries for numerical computation and the Matplotlib library for visualization. Convex hulls were computed using SciPy’s implementation of the Quickhull algorithm.

Random arrangements were generated by applying the Fisher-Yates shuffle to the array $[1, 2, \dots, n^2]$ and reshaping to an $n \times n$ grid. This procedure samples uniformly from the $n^2!$ possible arrangements.

Magic squares were generated using classical construction methods: the Siamese (de la Loubère) method for odd orders ($n = 3, 5$) and the doubly-even diagonal method for $n = 4$. This choice of methods ensures that we test the framework across both parity classes, which differ in their geometric structure (presence or absence of a central cell) and construction algorithms. The zero-covariance property was verified to hold within floating-point precision (typically $< 10^{-14}$) for all generated magic squares of all three orders.

Source code for all analyses and figures is available in the supplementary materials. An interactive web application for visualizing Magic Gems is available at <https://kylemath.github.io/MagicGemWebpage>

A.6 Summary Statistics

Section 4 summarizes key statistics for magic squares of orders 3, 4, and 5.

n	Arrangements	Magic Squares	Equiv. Classes	Probability	$M(n)$
3	3.6×10^5	8	1	2.2×10^{-5}	15
4	2.1×10^{13}	7,040	880	3.4×10^{-10}	34
5	1.6×10^{25}	2.8×10^8	3.4×10^7	1.8×10^{-17}	65

Table 4: Statistics for magic squares of orders 3, 4, and 5, showing the total number of arrangements, number of magic squares, number of equivalence classes under D_4 , probability of a random arrangement being magic, and the magic constant $M(n)$.